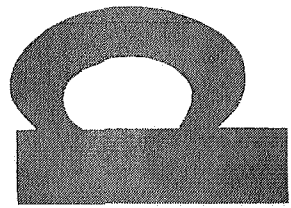WYLE LABORATORIES - RESEARCH STAFF

TECHNICAL MEMORANDUM 68-3

EXPERIMENTAL STUDY OF
SHOCK-PANEL COUPLING -
PRELIMINARY RESULTS

WYLE LABORATORIES
TESTING DIVISION, HUNTSVILLE FACILITY

research

WYLE LABORATORIES - RESEARCH STAFF

TECHNICAL MEMORANDUM 68-3

EXPERIMENTAL STUDY OF
SHOCK-PANEL COUPLING -
PRELIMINARY RESULTS

By

J. A. Cockburn

Work Performed Under Contract NAS8-21100 DCN-1-75-20062
Aerodynamic Noise Research

Principal Investigator - M. V. Lowson

March 1968

COPY NO. ___4

SUMMARY

An experimental investigation to determine the significance of shock-panel coupling is described. A flexible panel subjected to supersonic turbulent flow was mechanically driven by an impedance head with and without a shock formed at the panel 1/2 chord position. The experimental results show that the presence of the shock causes a large increase in the modal stiffness, or impedance, of the panel which is not fully accounted for by the contribution from the static pressure behind the shock. A simple analysis, based on propagation of disturbances through the shock by panel motion, suggests that for low order modes shock-panel coupling can either amplify or resist panel motion, depending on the free stream Mach number, panel dimensions, vibratory mode and resonant frequency. However, it is not sufficiently clear whether the observed increase in modal stiffness is due to coupling or to increased damping caused by the separated flow. To clarify this point, and to investigate further the shock-panel coupling mechanism, additional experimental work covering a wide range of modal frequencies and flow Mach numbers is recommended.

TABLE OF CONTENTS

LIST OF FIGURES

1.0 INTRODUCTION

A recent study of shock interactions with turbulence and sound (reference 1) has shown that sound waves impinging on a shock are increased in intensity behind the shock. A separation shock at Mach 2 was shown to increase the sound intensity by about 4.5 dB and it was concluded from this study that inter-action of a shock wave with local panel motion could be a significant effect. It was suggested that the shock might easily act as a "sounding board" for such panel motions and possibly lead to some form of shock-panel instability. In an attempt to further investigate this mechanism, a number of shock-panel coupling experiments were defined. The purpose of these experiments was twofold; firstly, to verify the existence of such a shock-panel coupling mechanism, and secondly, to obtain a quantitative description of the panel response and the induced pressure levels at the panel surface immediately behind the shock.

In this Memorandum, a preliminary experiment, which was performed in order to verify the existence of the shock-panel coupling mechanism, is described. The experiment involved setting up a flexible panel in the wall of a supersonic wind tunnel, mechanically exciting the second mode (by means of an impedence head) with and without a shock formed at the 1/2-chord point, and measuring the force and acceleration at the driving point. A second experiment, involving mechanical excitation of the first mode with the shock placed at the downstream edge of the panel, was planned as a means of satisfying the second objective outlined above; however, because of problems with the panel edge fixity, repeatability, and the instrumentation, it was not possible to complete this experiment in the available time.

2.0   EXPERIMENTAL APPARATUS

The experiments were carried out in the NASA 7-inch supersonic tunnel facility at the Marshall Space Flight Center. This tunnel has an operating Mach number range of 1.54 to 5; the dimensions of the test section are shown in Figure 1 and a table of aerodynamic constants is given in Figure 2. The Mach number chosen for the present investigation was Mach 2.44.

The test panel consisted of a 6 1/2-in. by 4 1/2-in. by 0.016-in. thick Titanium Alloy sheet flush-mounted in the removeable tunnel sidewall such that the effective panel dimensions were 5 in. in the flow direction and 3 in. transverse flow. Flush-mounting of the panel into the tunnel sidewall was achieved by use of screws, shims and epoxy bonding, as shown in Figure 3. To obtain separated flow and the formation of a shock, several sets of tapped holes were provided in the removeable sidewall to accommodate a 4-in. by 1-in. by 3/4-in. steel block. A photograph of the block, showing the mounting on the tunnel sidewall relative to the test panel, is shown in Figure 4. Preliminary experiments, using china clay for flow visualization were necessary to establish the positions of the tapped holes in the tunnel sidewall for precise location of the shock in subsequent experiments. Mechanical excitation of the panel was accomplished by use of a Wilcoxon Z602 impedance head; the head could be cemented to any desired point on the panel through a 1/2-in. diameter contacting surface and its effective weight counterbalanced by suspending an equal weight from a cord connected to its center of gravity.

The electronic apparatus used in this investigation is shown in the block diagram of Figure 5. Due to difficulties in the phase plotting system, the force and acceleration signals were recorded on tape from the output of the tracking filters, together with a frequency signal from the sweep oscillator, for subsequent determination of the phase lag between them.

2

3.0 EXPERIMENTAL PROCEDURE

3.1 Structural Characteristics of the Panel.

With the test panel assembled in the tunnel and the test section open to atmosphere, the impedance head was attached to the 1/4-chord point on the centerline of the panel and a sinusoidal sweep from 100 Hz to 1000 Hz performed. Several frequency sweeps were performed to examine the effects of maintaining force, acceleration and oscillator output voltage constant. Very little difference was observed between the three different test methods, however, since oscillator output voltage was the most convenient parameter to maintain constant, all subsequent frequency sweeps were carried out in this manner. Frequency sweeps, at constant oscillator voltage, were repeated several times to establish the resonant frequencies, damping in each mode and the overall repeatability. The effects of increasing the force amplitude on the acceleration response during dwell tests in the first and second modes were also studied; these tests showed that over the same force range the first mode response was significantly more linear.

3.2 Attached Flow.

For this series of tests, the panel was mechanically driven at the 1/4-chord point while flow in the tunnel at Mach 2.44 was maintained. Initially the mechanical excitation consisted of a frequency sweep through the second mode but in view of the superimposed random response on the sinusoidal data and the consequent lack of resolution, the sweep was discontinued in favor of a resonance dwell in the second mode. During the dwell test, force and acceleration were plotted and the fluctuating pressures beneath the turbulent boundary layer at the downstream edge of the panel were monitored.

3.3 Separated Flow.

Several preliminary runs were performed at Mach 2.44, with china clay applied to the panel for flow visualization, while varying the position of the steel block so as to form the shock exactly at the 1/2-chord point. Once the block position was fixed, the panel was mechanically driven in its second mode while flow in the tunnel at Mach 2.44 was maintained. Force and acceleration were plotted and the fluctuating pressures beneath the boundary layer at the downstream edge of the panel were monitored.

4.0   DISCUSSION OF RESULTS

The variation of force and acceleration as a function of excitation frequency is shown in Figure 6. This result was obtained with the impedance head attached to the 1/4 chord point. The first, second and third modes (i.e., 1,1   2,1 and 3,1) have resonant frequencies of 360 Hz, 600 Hz and 720 Hz respectively. The irregularity observed at 500 Hz is most probably associated with the transition from one flexural half-wave to two flexural half-waves along the flow direction. During this transition period, a point on the 1/2-chord line oscillates about the equilibrium position with decaying amplitude before taking up the position of a node. This irregularity would normally be attributed to "oil-canning" of the panel, though frequent examination throughout the tests revealed no permanent set or varying tension. However, upon completion of the experimental program when the tunnel sidewall was removed, a failure of the bonding along almost the whole of the long panel edge was observed; in spite of this failure it was still possible to excite the panel modes with the impedance head. It is therefore possible that the bonding failure occurred during the initial stages of the experiment and contributed to the non-linearity at 500 Hz.

The overall response plot is disappointing since only the first and third modes are well defined; this clearly points out the difficulties associated with mechanical excitation of flexible panels. The Wilcoxon Z602 impedance head used in this study was rated at 3/4 lb. maximum "blocked" force output. Due to the flexibility of the test panel, the maximum available force from the driver was very much less than this figure; in fact the measured forces and accelerations when compared with the manufacturers minimum recommended impedances show that the experimental range investigated was only marginally above the noise floor of the transducer. Subsequent experiments in this area will obviously require a substantially stiffer panel and/or impedance head with a maximum rated "blocked" force output somewhat less than 3/4 lb.

The linearity of the acceleration response is illustrated in Figures 7(a) and 7(b) which present the force and acceleration data for the first and second panel modes respectively. The experimental conditions applicable to each data point are indicated in the figure.

Some scatter is evident, caused possibly by temperature effects across the panel due to aerodynamic heating, but the figures show that in general the response is more linear in the first mode. The modal stiffnesses over the linear portions, calculated approximately from the resonant frequencies, acceleration and force levels, are about 13 lb./inch and 350 lb./inch for the first and second modes respectively and typical values of Q (averaged from all tests) were 35 and 50 respectively.

The results of a dwell test at the second panel resonance, while the tunnel was operated at a Mach number of 2.44, are indicated by points A and B in Figure 7(b). During this test run, the overall sound pressure level, monitored by the transducer

4

at the aft edge of the panel, was 138 dB re 0.0002 dynes/cm^2.

The result of a similar dwell test with a shock formed at the 1/2-chord point, is shown by the point C in Figure 7(b). It is clear that the effective stiffness of the panel, and thus the impedance, increases considerably for this structural mode due to the presence of a shock. Also, the overall sound pressure level monitored by the transducer was found to have increased to 158 dB re 0.0002 dynes/cm^2. An approximate calculation based on the geometry of the step and the tunnel aerodynamic parameters suggests that a static pressure of the order of 0.65 lb./in^2 is present over the rear half of the panel, which would tend to increase the effective panel stiffness. From Figure 7(b), the effective panel stiffness for the second mode in the presence of a shock is about 1900 lb./in. Using simple plate theory, the 0.65 lb./in^2 loading over the rear half of the panel is found to be equivalent to an additional stiffness of about 210 lb./in. Assuming that this latter stiffness acts in parallel with the panel stiffness in the absence of a shock (i.e., 350 lb./in) the overall effective stiffness increases to about 560 lb./in, which is considerably less than the 1900 lb./in computed from the experimental data. Clearly some form of coupling has taken place, though it is difficult to ascribe the increased stiffness to a particular mechanism at this stage. For example, the stiffness at resonance is wholly quadrature and therefore a measure of the damping, so that additional damping introduced by the separated flow may well account for this increase; alternatively, the propagation of velocity disturbances through the shock which couple with the rear half of the panel could also account for the increase. It is worthwhile to consider the latter mechanism in more detail and examine the tunnel and structural parameters which could be of significance. In the following discussion, a simple analysis of shock-panel coupling via velocity disturbances is presented.

4.1   Simple Analysis of Shock-Panel Coupling.

In this discussion it is assumed that the basic mechanism for the shock-panel coupling can be described as follows:

i)   The vibratory panel motion causes a wave to be formed in the free stream in front of the shock which is related to the panel motion.

ii)   This wave is convected through the shock at the mean flow velocity external to the boundary layer.

iii)   The amplified pressure wave behind the shock causes forced motion of the panel.

The object of introducing this simplified model is to reveal some of the key features that might be expected in practice. Clearly, many features have been ignored, and several of those must be expected to be of significance. Nevertheless, it is thought that this simple theory is of some value in interpreting the present experi-

5

mental results. Mathematical models are introduced in the following analysis but these are intended as an aid to discussion, rather than for any calculation purposes.

Suppose that the panel velocity, in a single normal mode (n) is given by

$$v_p = \text{Re}\left(v_n \, \sin \, k_n x \, \exp. \, i \, \omega_n \, t\right) \tag{1}$$

which is representative of the axial modes of a simply-supported panel. This motion is assumed to give rise to a wave in the air which is convected along at an axial velocity of u_o; the appropriate form for the wave velocity is:

$$v_a = \text{Re}\left[v_n \, R \, \sin \left\{ k_n \, u_o \left(t - \frac{x}{u_o}\right)\right\} \exp. \left\{ i \, \omega_n \left(t - \frac{x}{u_o}\right)\right\}\right] \tag{2}$$

where R is a complex transfer function which includes phase and amplitude effects as a result of the transfer from the panel to the air.

After passing through the shock, the axial velocity of the wave in the air will be modified to u_1 and the pressure behind the shock may be described by

$$p = \text{Re}\left[v_n \, RS \, \sin \left\{ k_n^1 \, u_1 \left(t - \frac{x}{u_1}\right)\right\} \exp. \left\{ i \, \omega_n \left(t - \frac{x}{u_1}\right)\right\}\right] \tag{3}$$

where the wave number k_n has been modified to k_n^1 because of the axial velocity change. If the velocity were reduced, then the wave number would increase since $k_n^1 \, u_1 = k_n \, u_o$. In Equation (3), S is the complex transfer function between v_a and p.

The above pressure can be assumed to act on the panel behind the shock. To calculate the mean panel response, Equation (3) must be integrated over time and over the panel area behind the shock. Clearly these are two important effects to consider;

i)   If $k_n \, u_o = \omega_n$, then the pressure wave arriving behind the shock has the same basic frequency as the panel response, and according to whether or not the wave is in or out of phase, it will amplify or resist the panel motion. However, if $k_n \, u_o \neq \omega_n$, then over a long time period the effects would be expected to cancel out.

ii)   Wavelength matching of the convected pressure wave and the panel structural wave. If the panel couples with the convected pressure wave then the magnitude of the coupling will be determined by the overall "acceptance" of the panel which is the spatial integral of the pressure waveform over the modal waveform of the relevant panel resonance. If any significant difference in wavelength between the

6

convected pressure wave and the panel wave exists then the result of this integration would be very small. Also, the higher order structural modes, having several wavelengths behind the shock, are particularly unlikely to be excited by the pressure wave. Furthermore, the greatest probability of panel coupling occurs as u_o approaches u_1.

It should also be borne in mind that small variations in the magnitude of $k_n u_o$ about ω_n will still lead to some coupling through damping, the magnitude of which will, of course, depend upon the response bandwidth of the particular panel mode.

A crucial point in the application of this discussion is the determination of u_o and u_1, the assumed speeds of the travelling waves. Associating u_o with the free stream velocity would only be valid if vorticity disturbances were created in the mainflow by the panel motion, which is not the case. It is possible, however, for the panel to generate disturbances in the boundary layer, in fact "viscosity waves" of this type are often considered in panel flutter studies to travel at 0.6 to 0.8 times the free stream Mach number. Perhaps the most realistic disturbance mechanism is an acoustic disturbance in the external stream. The generalized acoustic disturbance resulting from an arbitrary panel vibration would be an extremely complicated "standing wave" type of pattern caused by interference between the various parts of the panel motion, including the double retarded time effects typical of supersonic flow. If the panel vibration is of low frequency, or the flow is of high Mach number, then the disturbances are propagated along "Mach lines" in a similar manner to propagated waves from a "wavy" wall; the axial transport Mach number is then given by $(M^2-1)/M$. It is of interest to note that this transport velocity lies in the same range as the viscous wave speed, i.e., between about 0.6 and 0.8 times the local Mach number for $1.6 < M < 2.2$, so that some reinforcement of the viscous wave may occur.

For convection velocities behind the shock, theory (Reference 1) shows that the sound wave generated by a velocity disturbance is usually at a small angle to the shock. The local convection Mach number behind the shock will therefore be greater than the local flow Mach number; thus it appears that for low supersonic speeds u_o and u_1 will be of the same order, and, as discussed above, this could be expected to lead to particularly efficient coupling.

It may be noted that the proposed coupling mechanism is different from those used elsewhere in panel flutter problems. A brief review of the literature on panel flutter showed that shock wave interactions were generally not considered. (References 2 and 3).

Ellen (Reference 4) has studied panel instability caused by oblique shock waves by linearizing the steady shock equations and obtaining a point function relationship between the local panel slope and the surface pressure. Longitudinal changes in shock foot position, caused by panel deflection, are assumed to be of negligible importance and it is also implied that waves from the shock-expansion interaction

7

have negligible effect on the surface pressure distribution as given by the linearized approximation. This approach is very different from that suggested here; however, results are presented which suggest substantial lowering of the flutter boundaries, even for weak shocks, when the shock is at a forward position on the panel. Furthermore, this mechanism could cause coupling at any input frequency so that the temporal coincidence effects discussed above would not occur.

Applying the condition (from the above analysis) that $k_n u_0 = \omega_n$ to the second mode, (i.e., $u_0 = \dfrac{2Lf_n}{n}$ where L = panel length, f_n = resonant frequency of the n-th mode and n = number of elastic half waves) predicts u_0 = 250 ft./sec for maximum efficiency of coupling which is substantially less than the value of 1600 ft/sec estimated for the flow Mach number investigated. This result suggests that the experimental condition investigated, i.e., Mach 2.44 and panel second mode, does not coincide with a strong shock-panel coupling mode. The observed large increase in panel stiffness is therefore not fully accounted for by this analysis and it might therefore be expected that the additional damping introduced by the separated flow was a contributing factor or alternatively, the frequency-independent mechanism proposed by Ellen had a significant contribution. Clearly, further experimental studies involving the variation of Mach number for a number of panel modes are required to verify the shock-panel coupling analysis and "coincidence" conditions predicted.

5.0   CONCLUSIONS AND RECOMMENDATIONS FOR FURTHER WORK

Mechanical excitation of the panel in its second mode with a shock formed at the 1/2-chord results in an observed increase in modal stiffness (or impedance) which is not fully accounted for by the contribution from the static pressure behind the shock, thus suggesting the existence of a shock-panel coupling mechanism. A simple analysis based on the propagation of disturbances through the shock by panel motion suggests that, in general, for the first few modes, shock-panel coupling can either resist or amplify panel motion depending on the values of the free stream Mach number, panel dimensions, and the forced vibratory mode and its resonant frequency. Following from the simple analysis, application of the criterion for shock-panel coupling suggests that the flow Mach number and panel mode investigated do not coincide with those which would result in a strong shock-panel coupling mode. The experimentally observed increase in panel stiffness is therefore not fully accounted for by the present analysis, suggesting that additional damping introduced by the separated flow was a contributory factor. Further experimental and theoretical studies are required to verify the proposed shock-panel coupling model and predict the "coincidence" conditions, or strong coupling modes.

In particular, it is recommended that in future experiments;

a)   panel stiffness should be increased and/or an impedance head rated considerably below 3/4 lb. maximum blocked force be used.

b)   the possibility of using a magnetic exciter and a non-contacting displacement transducer be investigated.

c)   closer attention should be paid to panel-bonding; the provision of a large number of screws appears to be preferable to epoxy bonding.

d)   the effects of exciting the panel at the 1/2-chord point and monitoring the pressure fluctuations at the downstream edge of the panel, as a function of the driving force, should be investigated since this should lead to a direct quantitative assessment of the shock-panel coupling mechanism.

e)   panel "oil canning" due to temperature effects caused by aerodynamic heating and damping effects caused by separated flow should be investigated.

f)   a range of panel thicknesses should be investigated, thus giving a wide frequency variation for the same panel modes; in conjunction with a range of Mach numbers, this should increase the probability of encountering strong shock-panel coupling modes.

REFERENCES

1. Lowson, M.V., "The Fluctuating Pressures due to Shock Interactions with Turbulence and Sound," Wyle Laboratories Research Staff Report WR 66-35, June 1966.

2. Fung, Y.C., "Some Recent Contributions to Panel Flutter Research," I.A.S. Papers No. 63-26 Presented at the 31st Meeting I.A.S. New York, January 1963.

3. Fung, Y.C., "Summary of the Theories and Experiments on Panel Flutter." AFOSR TN-60-224, Calif. Inst. Tech. May 1960.

4. Ellen, C.H., "Panel Instability Caused by Oblique Shock Waves," AIAA Journal, Vol. 4, No. 4, April 1966, pp. 680-688.
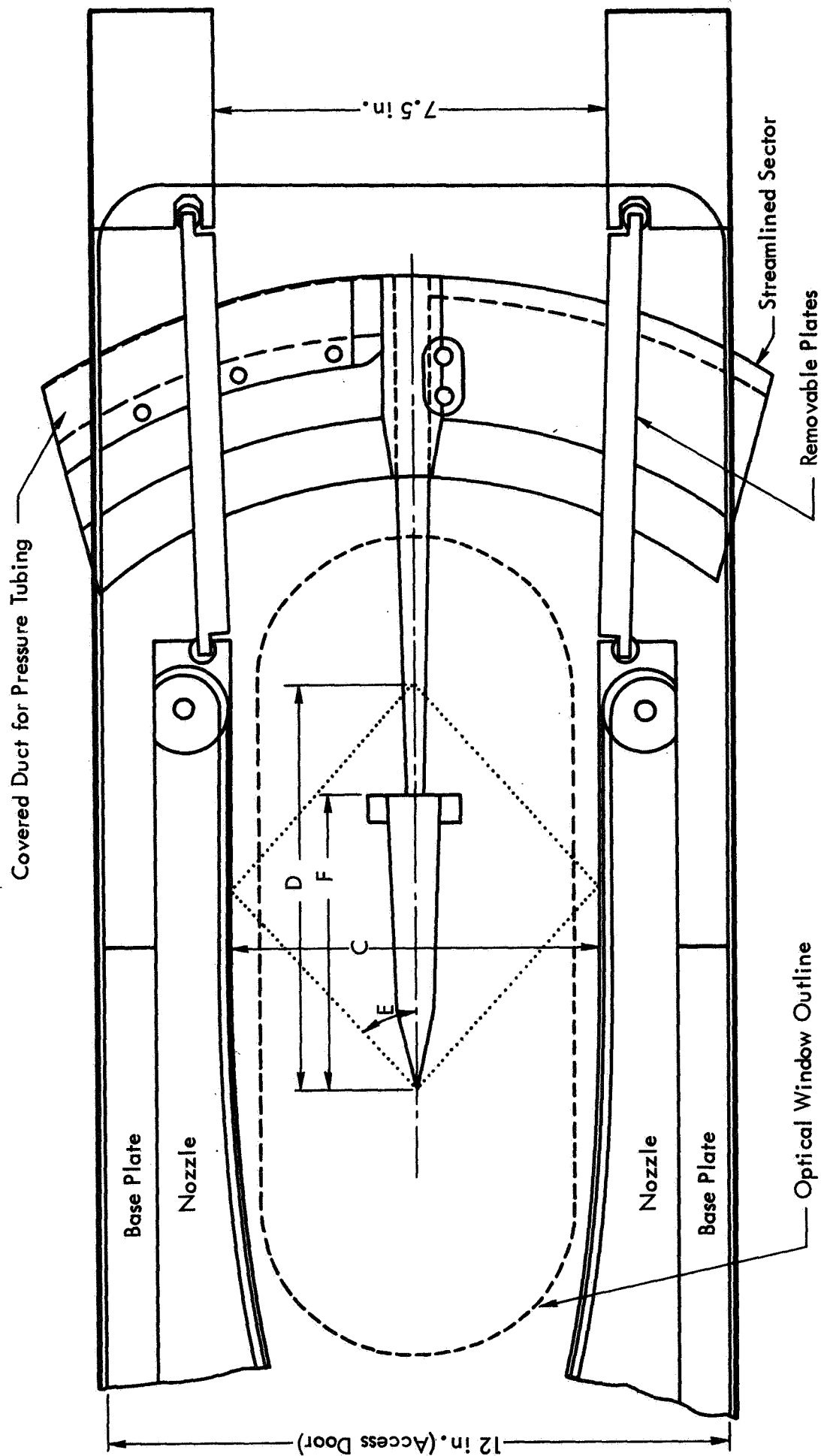
Figure 1. Test Section Dimensions

	1.54	1.99	2.44	3.00	3.26	4.00	5.00
Mach No.	1.54	1.99	2.44	3.00	3.26	4.00	5.00
Mass Flow (Lb./sec)	13.053	10.030	6.382	3.686	2.802	1.392	.576
Dynamic Pres. (psi)	6.26	5.29	3.94	2.52	2.03	1.08	.486
Static Pres. (psi)	3.78	1.91	.945	.400	.272	.097	.028
Mach Angle (Deg) "E"	40°30'	30°10'	24°12'	19°28'	17°52'	14°29'	11°32'
Length of Test Rhombus (in) "D"	8.871	12.913	15.985	19.395	22.495	27.100	35.571
Test Section Height (in) "C"	7.150	7.380	7.184	6.856	7.250	7.000	7.260
Throat Opening (in) "B"	5.522	4.250	2.964	1.560	1.186	.592	.236
Length of Nozzle (in) "A"	8.831	16.750	13.625	15.125	16.304	19.656	20.500
Length of Model (in) "F"	6.421	9.523	10	10	10	10	10
Reynolds No/In	360,353	305,185	250,000	185,608	163,971	111,306	82,216
Minimum Starting Pressure (psia) (Tunnel Clear)	10.6	9.25	6.55	5.41	5.01	1.65	.75
Maximum Run Time (sec)	183	210	225	332	378	425	391

Atmospheric Conditions P = 14.7 psia, T = 90° F, ρ = .0722 Lb./ft^3
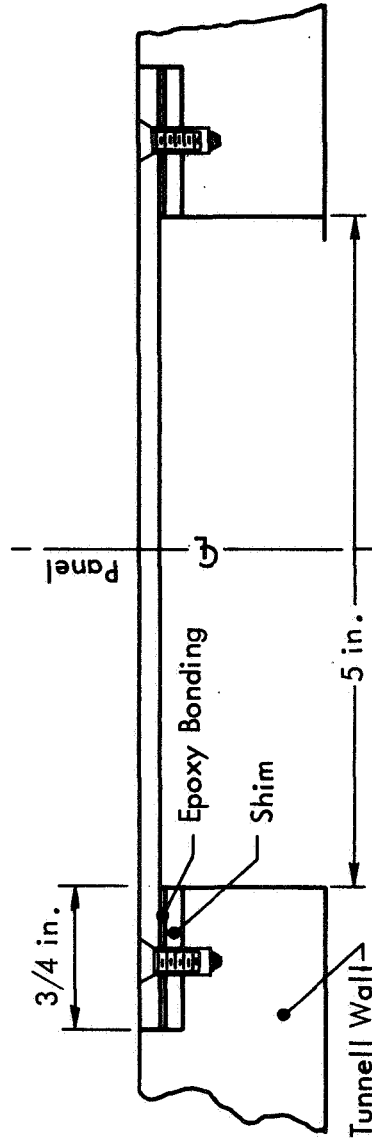
Figure 2. Table of Aerodynamic Constants

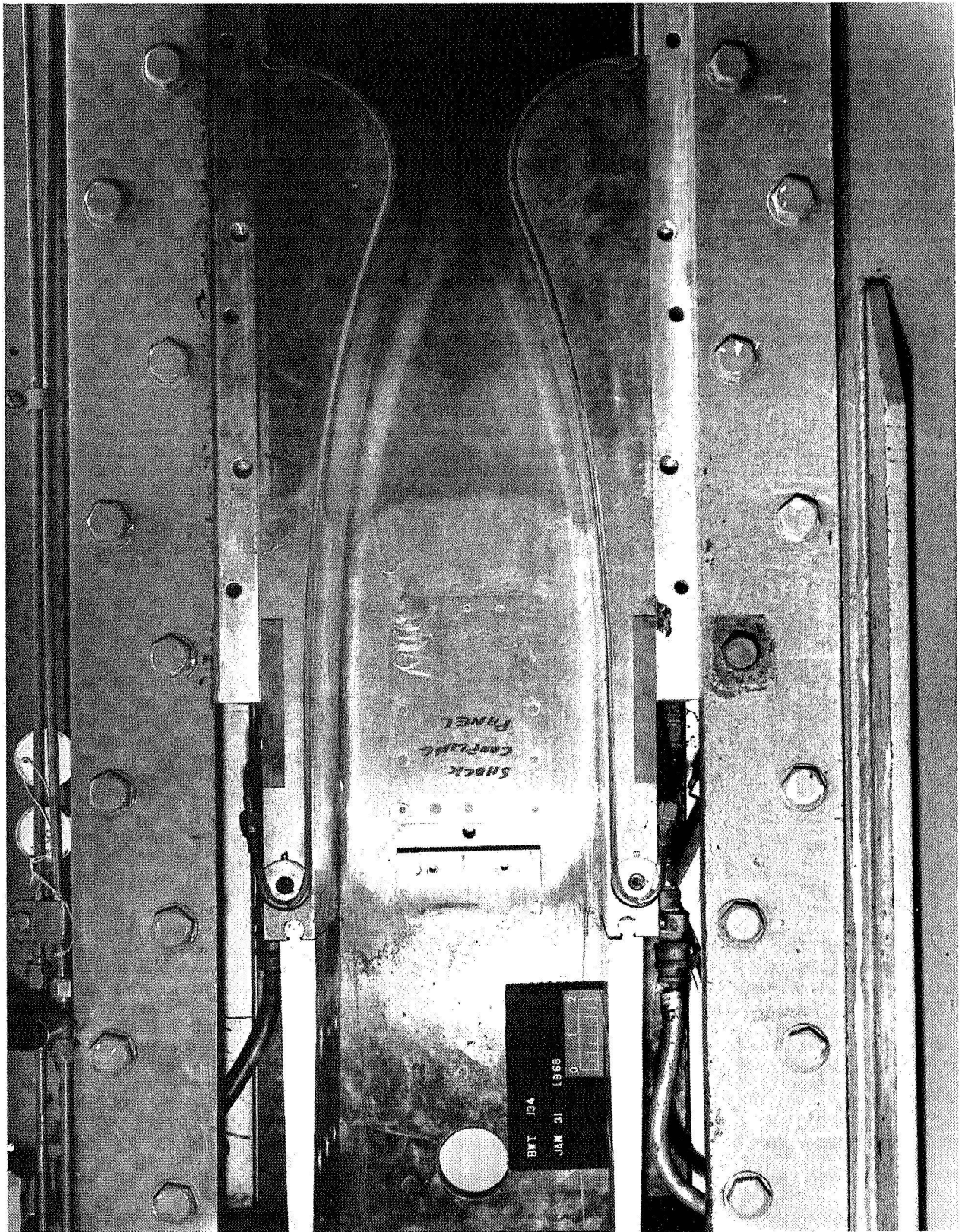Figure 3. Panel Mounting Arrangement.

13

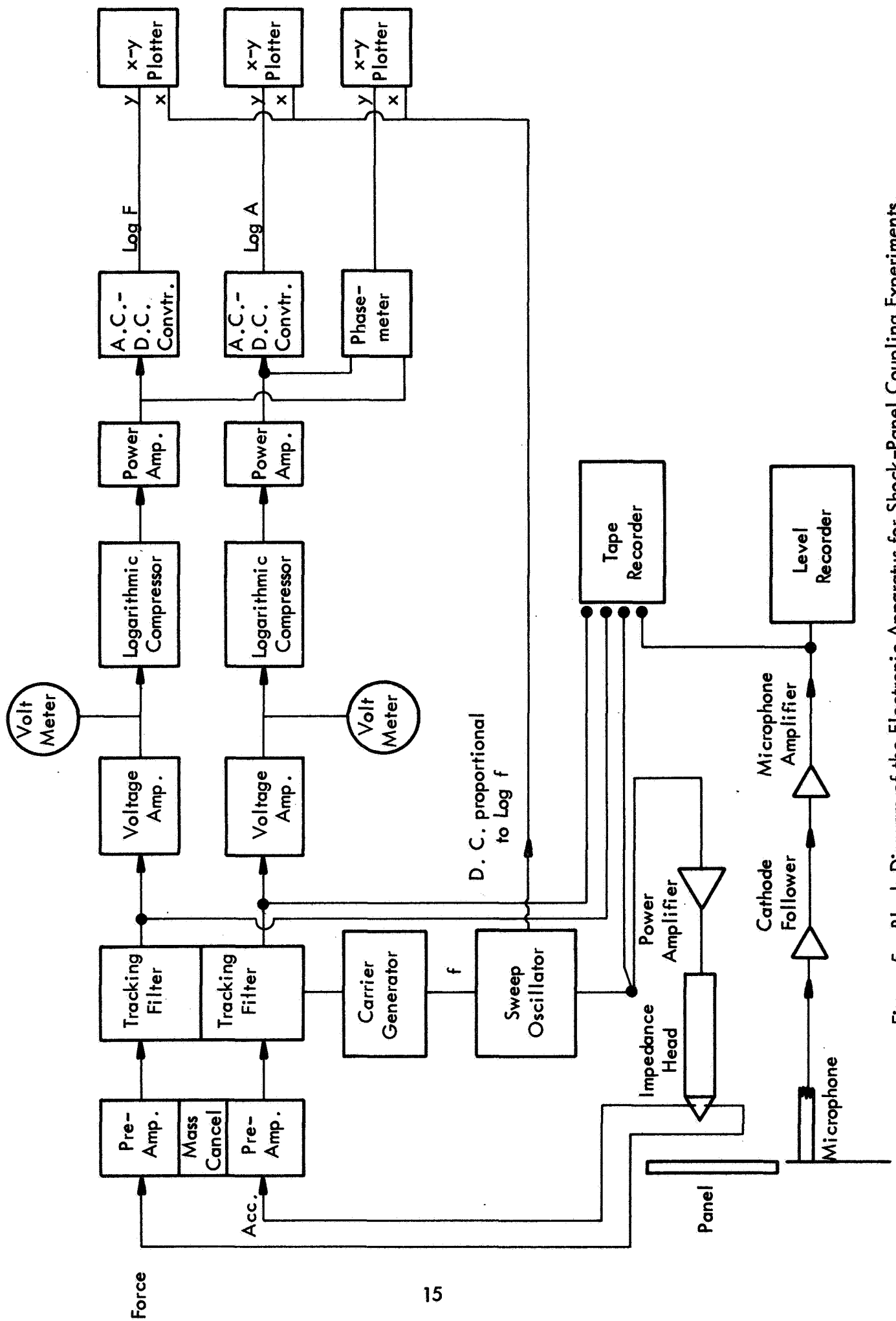Figure 4. View of the Test Section with the Panel and Step in Place.

Figure 5. Block Diagram of the Electronic Apparatus for Shock-Panel Coupling Experiments.
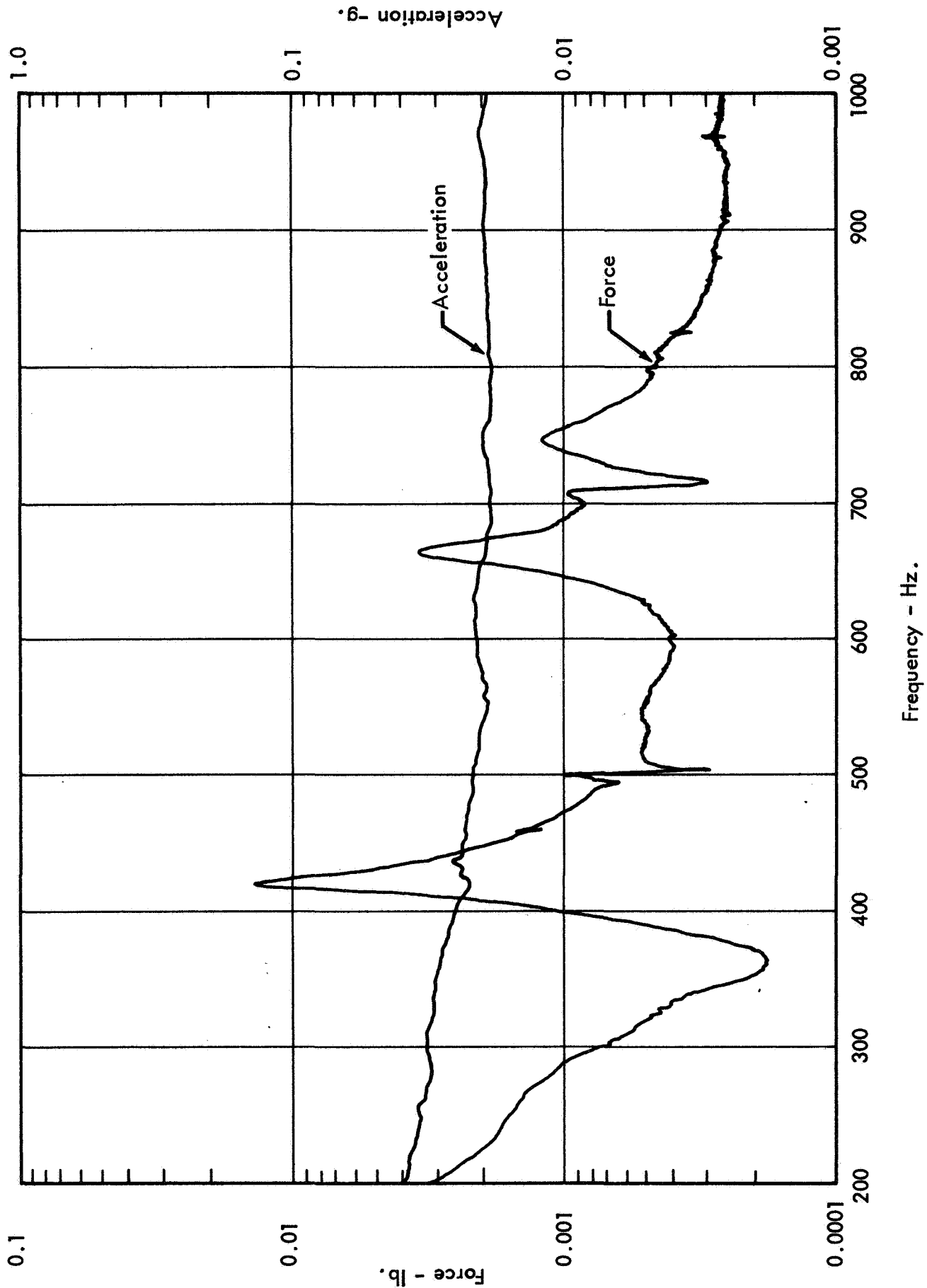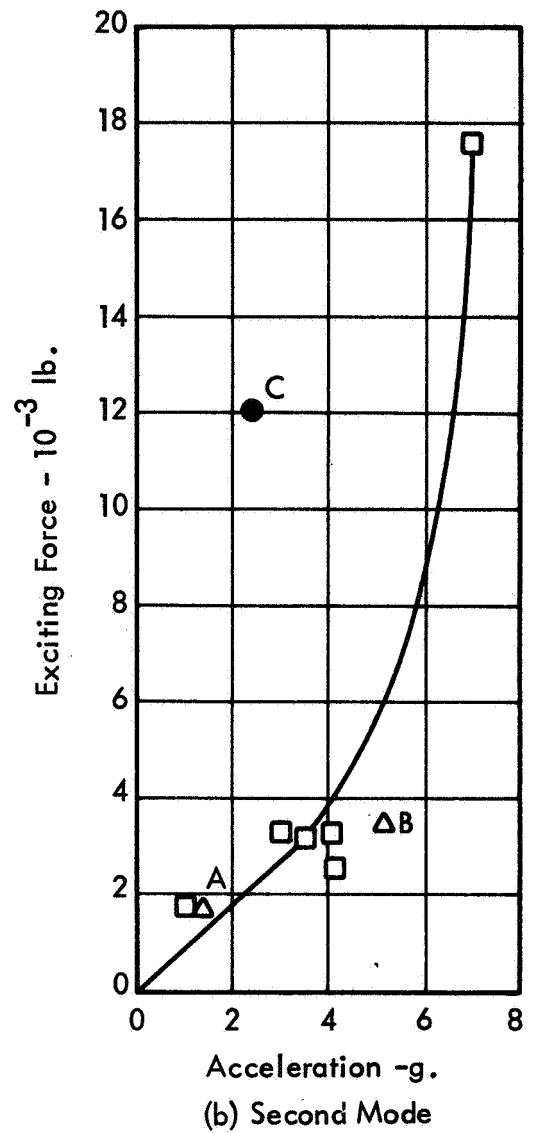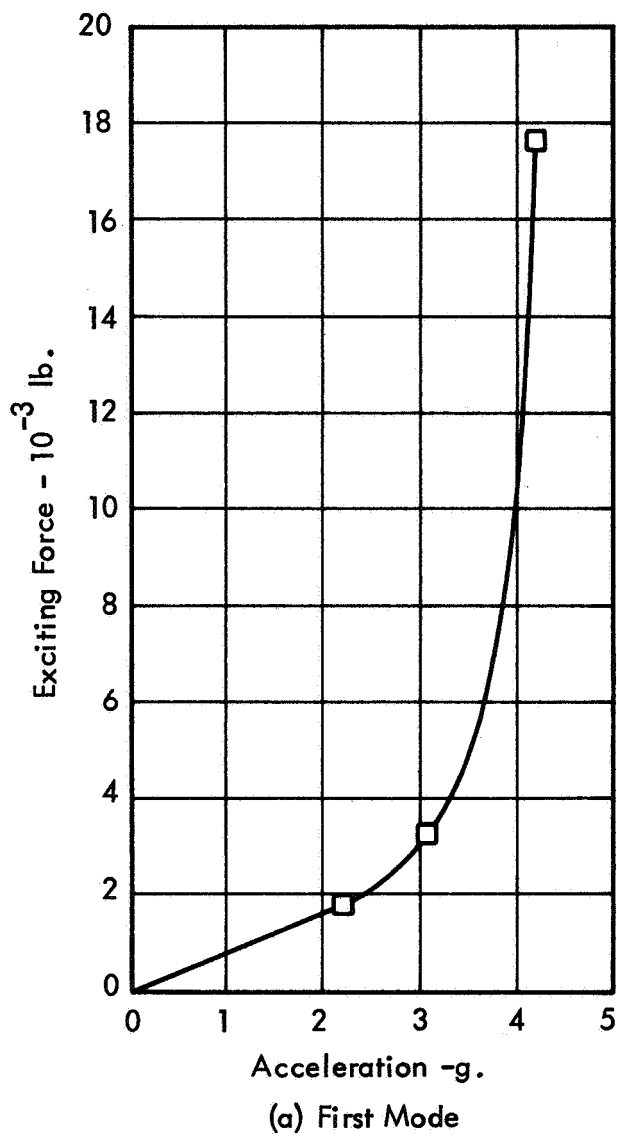
15

Figure 6. Force and Acceleration Response of the Panel versus Frequency.

16

Figure 7. Experimental Results Showing Linearity of the Panel Response and the Effects of Separated Flow.